



Total prompt energy release in the neutron-induced fission of ^{235}U , ^{238}U , and ^{239}Pu

D.G. Madland

Theoretical Division, Los Alamos National Laboratory, Los Alamos, NM 87545, USA

Received 12 January 2006; received in revised form 28 March 2006; accepted 29 March 2006

Available online 2 May 2006

Abstract

This study addresses, for the first time, the total prompt energy release and its components for the fission of ^{235}U , ^{238}U , and ^{239}Pu as a function of the kinetic energy of the neutron inducing the fission. The components are extracted from experimental measurements, where they exist, together with model-dependent calculation, interpolation, and extrapolation. While the components display clear dependencies upon the incident neutron energy, their sums display only weak, yet definite, energy dependencies. Also addressed is the total prompt energy deposition in fission for the same three systems. Results are presented in equation form. New measurements are recommended as a consequence of this study.

© 2006 Elsevier B.V. All rights reserved.

PACS: 24.75.+i; 25.85.Ec; 25.85.Ca; 27.90.+b

Keywords: Energy release and energy deposition in neutron-induced fission; Experiment and Los Alamos model; ^{235}U ; ^{238}U ; ^{239}Pu

1. Introduction

This study is a consequence of open questions on the magnitudes of the total prompt energy release in fission, the total prompt energy deposition in fission, the components of these quantities, and their dependencies upon the kinetic energy of the neutron inducing the fission. Our results are given in Eqs. (31)–(33) and Fig. 17 for the total prompt energy release in fission, and in Eqs. (46)–(48) and Fig. 23 for the total prompt energy deposition in fission. Recommended new experimental measurements coming from this study are given in Section 6. It should be noted that the study relies primarily upon existing published experimental measurements and secondarily upon

E-mail address: dgm@lanl.gov (D.G. Madland).

nuclear theory and nuclear models. Therefore, new and higher quality measurements would improve the results presented here and, furthermore, would lead to a more complete understanding of post scission fission physics.

2. Energy conservation

The energy release in fission is obtained from energy conservation. If one considers the binary fission of an actinide nucleus of mass number $A - 1$ induced by a neutron of mass m_n , kinetic energy E_n , and binding energy B_n in the compound nucleus A formed when the neutron is absorbed, then energy conservation gives

$$\begin{aligned} E_n + m_n + M(Z, A - 1) &= T + M^*(Z, A) \\ &= T_L(Z_L, A_L) + M_L^*(Z_L, A_L) \\ &\quad + T_H(Z_H, A_H) + M_H^*(Z_H, A_H), \end{aligned} \quad (1)$$

where the left side specifies the initial conditions prior to fission, the right side specifies the excited compound nucleus that is about to fission, and the second right side specifies the excited fission fragments just after binary fission has occurred. The notation here is that T is a compound nucleus or fragment kinetic energy, M and m are stable masses, M^* are masses of excited nuclei, all in units of MeV (c^2 has been suppressed), and L and H refer to the light and heavy fragments occurring in the binary fission.

The neutron binding energy B_n is obtained from the Q-value for neutron capture,

$$m_n + M(Z, A - 1) = M(Z, A) + B_n \quad (2)$$

which, when inserted into Eq. (1), yields

$$\begin{aligned} E_n + B_n + M(Z, A) &= T_L(Z_L, A_L) + T_H(Z_H, A_H) + M_L(Z_L, A_L) \\ &\quad + M_H(Z_H, A_H) + E_L^*(Z_L, A_L) + E_H^*(Z_H, A_H), \end{aligned} \quad (3)$$

where we have written an excited fragment mass as the ground-state mass plus the excitation energy, namely, $M^* = M + E^*$. This excitation energy will be dissipated by the emission of prompt neutrons and prompt gamma rays.

The *total energy release* E_r in binary fission is defined as the ground-state mass of the compound nucleus undergoing fission minus the ground-state masses of the two binary fission fragments, namely,

$$E_r = M(Z, A) - M_L(Z_L, A_L) - M_H(Z_H, A_H), \quad (4)$$

where (again) the masses are expressed in units of MeV [1]. This equation also defines the total energy release in each stage of multiple-chance fission except for the average kinetic and binding energies of the neutron(s) emitted prior to fission in each stage, which must be taken into account. Inserting Eq. (4) into Eq. (3) yields a second expression for the energy release in fission:

$$E_r = T_L(Z_L, A_L) + T_H(Z_H, A_H) + E_L^*(Z_L, A_L) + E_H^*(Z_H, A_H) - (E_n + B_n). \quad (5)$$

In these equations, conservation of charge ensures that $Z = Z_L + Z_H$, and conservation of baryon number ensures that $A = A_L + A_H$. Note that in Eq. (5) the kinetic and binding energy of the neutron inducing fission explicitly appear, with a minus sign, but they also implicitly appear in the fragment excitation energies E_L^* and E_H^* . And for spontaneous fission one replaces $(E_n + B_n)$ with 0, while for photofission the replacement is E_γ .

If we now sum the fragment kinetic energies and fragment excitation energies, Eq. (5) becomes

$$E_r = T_f^{\text{tot}} + E_{\text{tot}}^* - (E_n + B_n) \quad (6)$$

with

$$T_f^{\text{tot}} = T_L(Z_L, A_L) + T_H(Z_H, A_H), \quad (7)$$

$$E_{\text{tot}}^* = E_L^*(Z_L, A_L) + E_H^*(Z_H, A_H). \quad (8)$$

The above equations are for the specific binary fission $(Z_L, A_L) + (Z_H, A_H)$.

However, a large number of binary mass splits are energetically allowed and they have been observed throughout the pre-actinide, actinide, and trans-actinide regions [2]. In the vicinity of the uranium and plutonium isotopes the fission-fragment mass range is (approximately) $70 \leq A_f \leq 170$ and for each A_f there are 4 to 5 contributing isobars leading to between 200 and 250 different possible mass splits in binary fission (f stands for fragment). This means that the total energy release E_r , the total fission-fragment kinetic energy T_f^{tot} , and the total fission-fragment excitation energy E_{tot}^* , in Eqs. (4)–(8), must be replaced by their average values as determined by weighting with the independent fission-fragment yields Y_f , where

$$Y_f(Z_L, A_L) = Y_f(Z - Z_L, A - A_L) = Y_f(Z_H, A_H) \quad (9)$$

leading to

$$\langle E_r \rangle = M(Z, A) - \frac{\sum [Y_f][M_L(Z_L, A_L) + M_H(Z_H, A_H)]}{\sum Y_f} \quad (10)$$

$$= \langle T_f^{\text{tot}} \rangle + \langle E_{\text{tot}}^* \rangle - (E_n + B_n) \quad (11)$$

with

$$\langle T_f^{\text{tot}} \rangle = \frac{\sum [Y_f][T_L(Z_L, A_L) + T_H(Z_H, A_H)]}{\sum Y_f}, \quad (12)$$

$$\langle E_{\text{tot}}^* \rangle = \frac{\sum [Y_f][E_L^*(Z_L, A_L) + E_H^*(Z_H, A_H)]}{\sum Y_f} \quad (13)$$

and the sums are understood to be over either the light $\{L\}$ or the heavy $\{H\}$ fission-fragment yields. Thus, Eqs. (9)–(13) replace Eqs. (4)–(8) for the total energy release in binary fission. Note, again, that in the case of spontaneous fission E_n and B_n in Eq. (11) are set to zero, while in the case of photofission they are replaced with E_γ .

Extraction of the average total *prompt* energy release in fission from Eqs. (9)–(13) requires consideration of the time dependence of the fission process and the introduction of definitions related to that time dependence. A schematic of neutron-induced binary fission is shown in Fig. 1. The terms appearing in the figure, as well as others, are defined as follows:

Scission point: The time at which the fission fragments are unalterably determined [3]. Loosely, the time at which the neck snaps between the nascent fission fragments.

Fission fragment: Nuclear species existing at the scission point and just beyond, but prior to the emission of prompt neutrons and prompt gamma rays.

Fission fragment acceleration time: $\sim 10^{-20}$ [s] due to Coulomb repulsion.

Prompt neutron emission time: In the range $\sim 10^{-18}$ to $\sim 10^{-13}$ [s] based upon measurement of compound nucleus lifetimes and calculation.

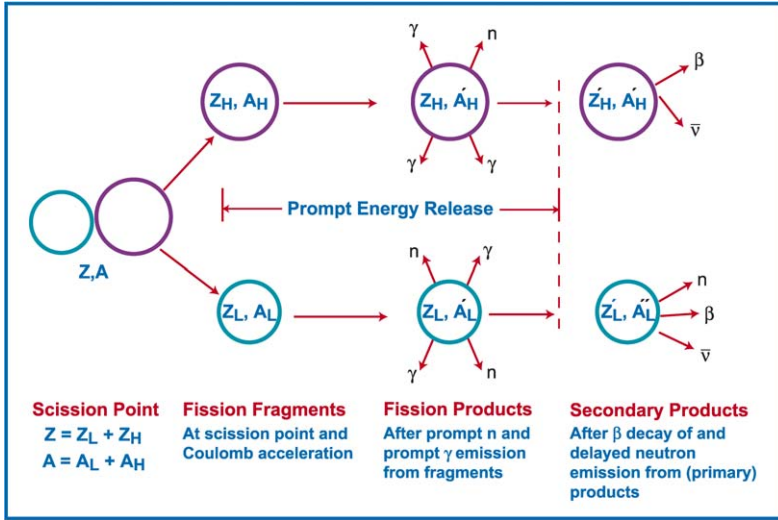


Fig. 1. Schematic of post scission in neutron-induced binary fission of target nucleus ($Z, A - 1$).

Prompt gamma emission time: In the range $\sim 10^{-14}$ to $\sim 10^{-7}$ [s] based upon time-of-flight measurements and calculation.¹

Prompt energy release time: In the range $\sim 10^{-20}$ to $\sim 10^{-7}$ [s].¹

Fission product (or *primary fission product*): Nuclear species existing following prompt neutron emission and prompt gamma emission from a fragment, but before any β decay has occurred.

Secondary fission product: Nuclear species existing following at least one β decay of a primary fission product. The shortest known fission-product β decay half-life is 0.032 [s]. Therefore, secondary fission products, β -decay energy spectra, antineutrino energy spectra, and subsequent delayed neutron energy spectra play no role in the total prompt fission energy release.

Now the independent fission-fragment yields $Y_f(Z_f, A_f)$ required in the solution of Eqs. (9)–(13) can only be obtained by construction from the measured independent fission-product yields $Y_p(Z_p, A_p)$ (where p stands for product), the measured average prompt neutron multiplicity as a function of fission-fragment mass $\bar{\nu}_p(A_f)$ (where p stands for prompt), and a Gaussian or Gaussian-like model assumption for the Z_f dependence of Y_f for fixed A_f . Note that $Z_p = Z_f$, but that $A_p \leq A_f$ due to the prompt neutron emission from the fragment. Furthermore, the independent fission-product yields $Y_p(Z_p, A_p)$ have been extensively measured, and tabulated, only for spontaneous fission and neutron-induced fission at two well-defined energies, thermal and 14 MeV (these are the well-known double-humped mass yield (A_p) distributions together with Gaussian charge yield (Z_p) distributions) [5]. Thus, solution of Eqs. (9)–(13) by use of constructed independent fission-fragment yields $Y_f(Z_f, A_f)$ is not currently tractable except for incident thermal neutrons and 14-MeV neutrons. Therefore, we turn to direct use of measured

¹ Note that the upper limit, $\sim 10^{-7}$ [s], may be application dependent and could, for example, be replaced by $\sim 10^{-8}$ or $\sim 10^{-6}$ [s].

and/or calculated values of the terms appearing in Eq. (11). Before proceeding we note the following:

Multiple-chance fission: Insofar as measured quantities are used in the evaluation of Eq. (11) the effects of multiple-chance fission are automatically taken into account. However, as will be seen, some calculated quantities are yet needed and these require multiple-chance fission treatment [see Eqs. (24) and (42)]. Appendix A contains the multiple-chance fission equations to be used in the calculation of the average total prompt fission energy release and energy deposition, $\langle E_r \rangle$ and $\langle E_d \rangle$ respectively, when none of the measured components of these quantities are available.

Ternary fission: For the incident neutron energy range $0 \leq E_n \leq 15$ MeV, approximately 1 in 500 fissions is ternary [6]. Therefore, ternary fission has been ignored in the preceding equations. However, insofar as ternary fission events have affected the measurements to be used below, their influence is present. Here, *ternary* means light charged particle accompanied fission.

Scission neutrons: The question of neutron emission at the scission point remains an open one, with experimental results ranging from 0% to 10% of the total average prompt neutron multiplicity $\bar{\nu}_p$ [6]. Measurements of this quantity, to be used below, include the scission neutrons if they exist.

Isomeric states: The de-excitation of fission fragments to (long-lived) isomeric states has been ignored in the preceding equations and time definitions. However, their effects are included insofar as they affect the measurements to be used below.

3. Components of the average total prompt fission energy release

The components of the average total prompt fission energy release $\langle E_r \rangle$ to be evaluated for the solution of Eq. (11) are the average total fission-fragment kinetic energy $\langle T_f^{\text{tot}} \rangle$ and the average total fission-fragment excitation energy $\langle E_{\text{tot}}^* \rangle$ whereas E_n and B_n are known. The largest component is the average total fission-fragment kinetic energy $\langle T_f^{\text{tot}} \rangle$ which becomes, after prompt neutron emission times ranging from 10^{-18} to 10^{-13} [s], the average total fission-product kinetic energy $\langle T_p^{\text{tot}} \rangle$ which is the measured quantity. More often than not, the experimentalists have converted the measured *product* kinetic energies back to *fragment* kinetic energies because they are more relevant to the development of fission theory. These quantities are related by the kinetic energies of the prompt neutrons emitted from the moving fragments as they become moving products. As a function of the kinetic energy E_n of the neutron inducing fission, one obtains

$$\langle T_p^{\text{tot}}(E_n) \rangle = \langle T_f^{\text{tot}}(E_n) \rangle \left[1 - \frac{\bar{\nu}_p(E_n)}{2A} \left(\frac{\langle A_H \rangle}{\langle A_L \rangle} + \frac{\langle A_L \rangle}{\langle A_H \rangle} \right) \right]. \quad (14)$$

Eq. (14) yields about a 2% kinetic energy correction due to prompt neutron emission from fully accelerated fragments coming from 14-MeV neutron-induced fission. The approximations used in its derivation are:

- (a) $m_n/M(Z, A) = 1/A$;
- (b) $\bar{\nu}_p(L) = \bar{\nu}_p(H) = \bar{\nu}_p/2$ where L and H refer to the average light and average heavy fragments;

- (c) $T_f/A = T_{f1}/(A - 1) = T_{f2}/(A - 2) = \dots$ where T_f is the initial fragment kinetic energy of the initial fragment A , and T_{fi} are fragment kinetic energies following the i th neutron evaporation from the moving fragment.

These approximations are sufficiently accurate to quantify a correction of order 2%.

The average total fission-fragment excitation energy $\langle E_{\text{tot}}^* \rangle$ is dissipated by two separate mechanisms: prompt neutron emission and prompt gamma emission, where *prompt* time has already been specified for each mechanism. Thus,

$$\langle E_{\text{tot}}^* \rangle = \langle Ex_n^{\text{tot}} \rangle + \langle E_\gamma^{\text{tot}} \rangle, \quad (15)$$

where the average fission-fragment excitation energy leading to prompt neutron emission is given by [4]

$$\langle Ex_n^{\text{tot}} \rangle = \bar{v}_p [\langle S_n \rangle + \langle \varepsilon \rangle] \quad (16)$$

with $\langle S_n \rangle$ the average fission-fragment neutron separation energy and $\langle \varepsilon \rangle$ the average center-of-mass energy of the emitted neutrons, and the average fission-fragment excitation energy leading to prompt gamma emission is given by $\langle E_\gamma^{\text{tot}} \rangle$. Eq. (11) now becomes

$$\begin{aligned} \langle E_r \rangle &= \langle T_f^{\text{tot}} \rangle + \langle Ex_n^{\text{tot}} \rangle + \langle E_\gamma^{\text{tot}} \rangle - (E_n + B_n) \\ &= \langle T_f^{\text{tot}} \rangle + \bar{v}_p [\langle S_n \rangle + \langle \varepsilon \rangle] + \langle E_\gamma^{\text{tot}} \rangle - (E_n + B_n). \end{aligned} \quad (17)$$

Note that all averaged quantities appearing in Eqs. (15)–(17) depend upon the incident neutron energy E_n which has been suppressed for brevity. We use Eq. (17) for the average total prompt energy release in neutron-induced fission for the remainder of this paper.

The existing experimental database for the neutron-induced fission of ^{235}U , ^{238}U , and ^{239}Pu , together with model-dependent interpolation, extrapolation, and calculation, allow a determination of $\langle E_r \rangle$ over the incident neutron energy range of $0 \leq E_n \leq 15$ MeV. However, as will be seen below, the experimental database is astonishingly incomplete. Where experiment does exist, we have performed linear or quadratic least-squares fits in E_n to the data and present the resulting parameters and their standard deviations in the following. Standard (theoretical) deviations in the Los Alamos model, as used in the following, are not quantitatively addressed herein.

3.1. Average total fission fragment and fission product kinetic energy

The experimental data that we use for the $n + ^{235}\text{U}$ system are those of Meadows and Budtz-Jorgensen (1982) [7], Straede et al. (1987) [8], and Müller et al. (1984, two data points only) [9]. The published fission-fragment (pre prompt neutron emission) total kinetic energies are shown in Fig. 2 and the corresponding fission-product (post prompt neutron emission) total kinetic energies, obtained with Eq. (14), are shown in Fig. 3. Linear fits to these data are also shown in the figures.

For the $n + ^{235}\text{U}$ system:

$$\langle T_f^{\text{tot}} \rangle = (170.93 \pm 0.07) - (0.1544 \pm 0.02)E_n \text{ (MeV)}, \quad (18)$$

$$\langle T_p^{\text{tot}} \rangle = (169.13 \pm 0.07) - (0.2660 \pm 0.02)E_n \text{ (MeV)}. \quad (19)$$

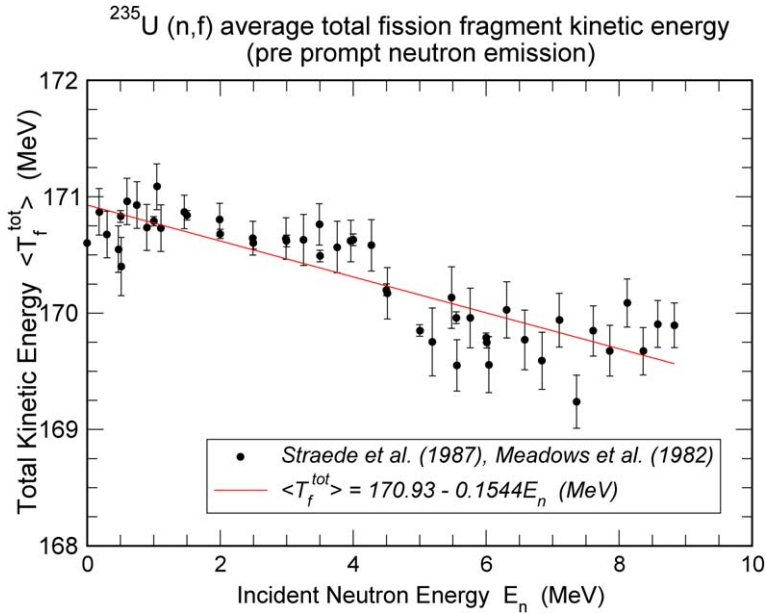


Fig. 2. Average total fission-fragment kinetic energy for the $n(E_n) + ^{235}\text{U}$ system.

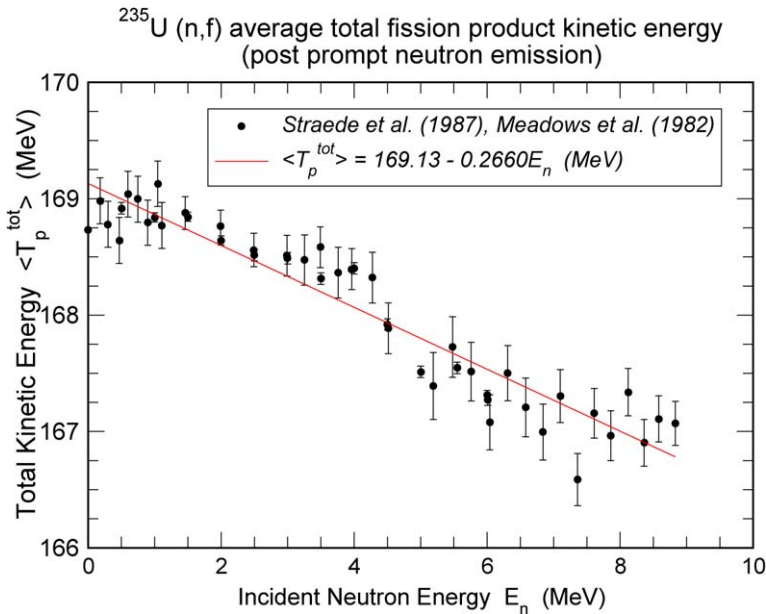


Fig. 3. Average total fission-product kinetic energy for the $n(E_n) + ^{235}\text{U}$ system.

The data appear to have structure (near the second-chance fission threshold, for example), but their scatter and uncertainties preclude anything other than a linear fit. The steeper negative slope for the total fission-product kinetic energy is due to the energy dependence of \bar{v}_p in Eq. (14). Strictly, Eqs. (18) and (19) should not be used above an incident neutron energy of about 9 MeV.

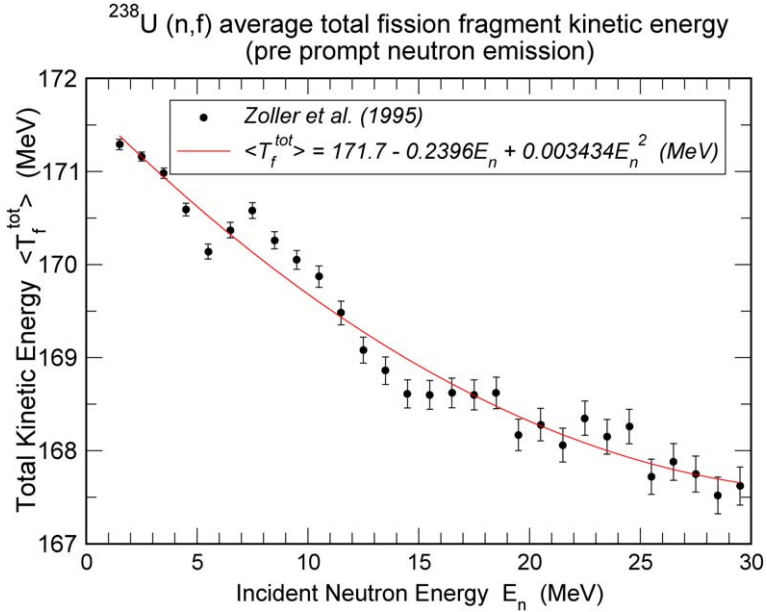


Fig. 4. Average total fission-fragment kinetic energy for the $n(E_n) + ^{238}\text{U}$ system.

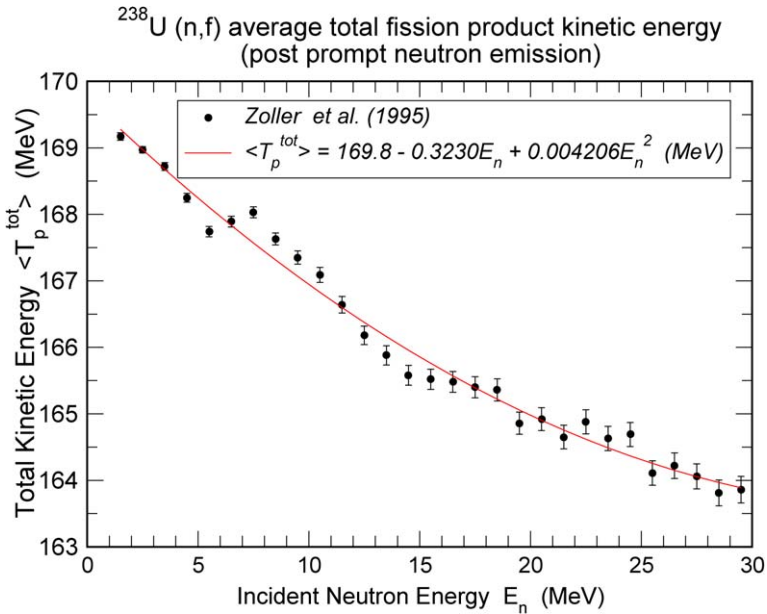


Fig. 5. Average total fission-product kinetic energy for the $n(E_n) + ^{238}\text{U}$ system.

The experimental data that we use for the $n + ^{238}\text{U}$ system are those of Zöller (1995) [10] shown in Figs. 4 and 5 for incident neutron energies up to 30 MeV. Here, the data give clear and convincing evidence for the presence of structure near the second- and third-chance fission

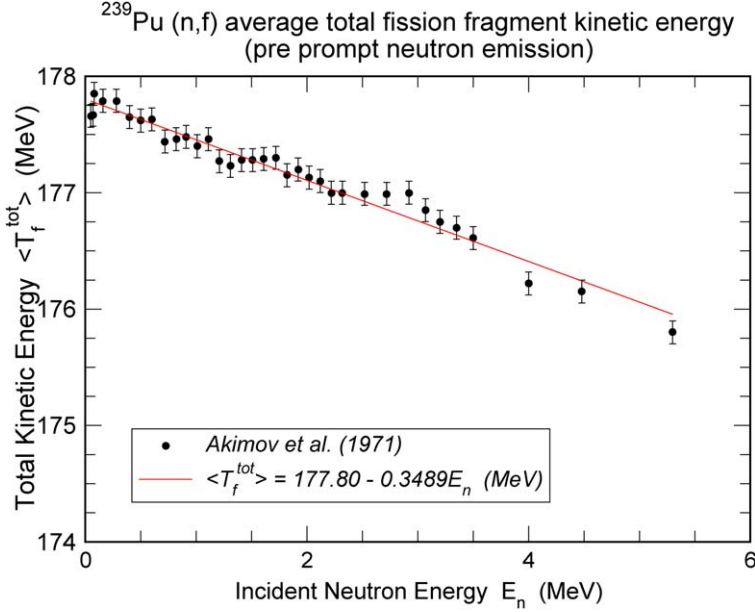


Fig. 6. Average total fission-fragment kinetic energy for the $n(E_n) + ^{239}\text{Pu}$ system.

thresholds. For our present purposes, however, we represent these data with quadratic fits for both the total fission-fragment and total fission-product kinetic energies because the corresponding experimental data for ^{235}U and ^{239}Pu are much lower in quality and over more limited energy ranges. We note that the recent experimental data of Vivès et al. (2000) [11] for this system, over an incident neutron energy range of 1.2–5.8 MeV, are in substantial agreement with the corresponding data of Zöllner (Fig. 4). The maximum discrepancy between the two measurements is $\sim 0.7\%$ at about 1.5 MeV.

For the $n + ^{238}\text{U}$ system:

$$\langle T_f^{\text{tot}} \rangle = (171.7 \pm 0.05) - (0.2396 \pm 0.01)E_n + (0.003434 \pm 0.0004)E_n^2 \text{ (MeV)}, \quad (20)$$

$$\langle T_p^{\text{tot}} \rangle = (169.8 \pm 0.05) - (0.3230 \pm 0.01)E_n + (0.004206 \pm 0.0004)E_n^2 \text{ (MeV)}. \quad (21)$$

The experimental data that we use for the $n + ^{239}\text{Pu}$ system are those of Akimov et al. (1971) [12] shown in Figs. 6 and 7 for incident neutron energies up to 5.5 MeV. Here, the data are not high enough in incident neutron energy to ask whether structure exists near the second-chance fission threshold.

Linear fits appear to be quite adequate for the limited energy range and, strictly, the fits should not be used above about 5.5 MeV. Note that in this system we have the steepest drop in the total kinetic energies with increasing incident neutron energy of the three systems under consideration.

For the $n + ^{239}\text{Pu}$ system:

$$\langle T_f^{\text{tot}} \rangle = (177.80 \pm 0.03) - (0.3489 \pm 0.02)E_n \text{ (MeV)}, \quad (22)$$

$$\langle T_p^{\text{tot}} \rangle = (175.55 \pm 0.03) - (0.4566 \pm 0.02)E_n \text{ (MeV)}. \quad (23)$$

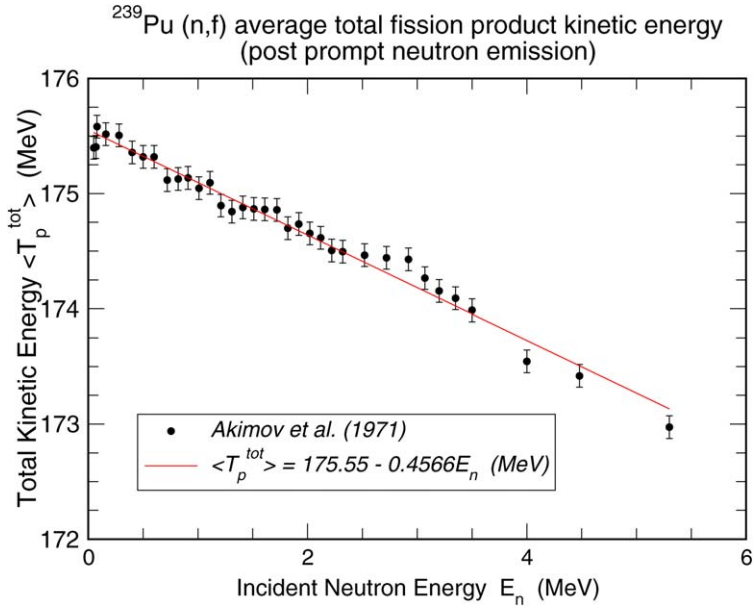


Fig. 7. Average total fission-product kinetic energy for the $n(E_n) + ^{239}\text{Pu}$ system.

For all three of these systems the average total fission-fragment and fission-product kinetic energies decrease with increasing incident neutron energy. The reason for this is that the fission-fragment yields for symmetric and near-symmetric fission are increasing with increasing incident neutron energy [2], but the total kinetic energies are at, or near, a minimum for symmetric and near-symmetric fission, thus decreasing the total kinetic energies with increasing incident neutron energy. This effect has been observed in experiment. See, for example, Fig. 11 of Ref. [13] for the $n(\text{thermal}) + ^{235}\text{U}$ system and Fig. 4 of Ref. [14] for the $n(\text{thermal}) + ^{239}\text{Pu}$ system. A (speculative) underlying physics reason for the observed effect may be that the charge centers of the nascent fission fragments are slightly farther apart for symmetric fission than they are for asymmetric fission.

The $n + ^{239}\text{Pu}$ system, $Z = 94$, has the largest kinetic energies of the three systems under study due to the Coulomb force, while those of the two U systems, $Z = 92$, are comparable to each other and somewhat less.

The fission product kinetic energies, in addition to being the *largest* component of the average total prompt energy release in fission, are the most *localized* in energy deposition having corresponding ranges, for example, of $\sim 5\text{--}10$ [microns] in uranium.

3.2. Average total prompt neutron emission energy

The average total prompt neutron emission energy is equal to the average fission-fragment excitation energy leading to prompt neutron emission ($\langle Ex_n^{\text{tot}} \rangle$) as given by Eq. (16). It is important to note that this quantity is not equal to the average total prompt fission neutron kinetic energy ($\langle E_{\text{neut}}^{\text{tot}} \rangle$) (to be discussed in Section 5) because (a) the portion of the prompt neutron kinetic energy due to the motion of the fission fragments emitting the neutrons has not yet been included and (b) the binding energy S_n of the neutron emitted does not contribute to the neutron kinetic energy.

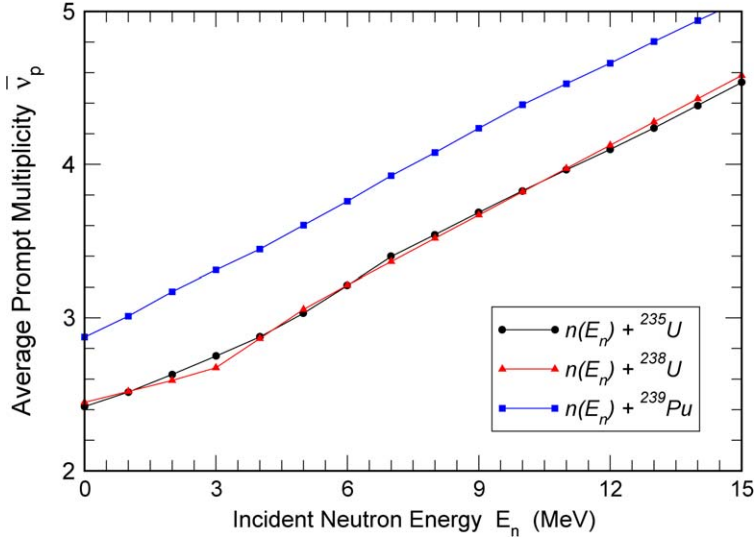


Fig. 8. Average prompt fission neutron multiplicity $\bar{\nu}_p$ for three systems from ENDF evaluated data (line segments are to guide the eye).

We evaluate Eq. (16) as a function of the incident neutron energy E_n as follows: First, the average prompt neutron multiplicities $\bar{\nu}_p(E_n)$ are taken from the ENDF evaluations [5] which are based upon experimental data. These are shown for the three systems under study in Fig. 8. Second, the average fission-fragment neutron separation energy $\langle S_n \rangle$ is calculated as one-fourth of the sum of the two two-neutron separation energies for a given binary mass split in a seven-point approximation to the light and heavy mass peaks, as described in Ref. [4], so as to average over two each of the four possible odd-particle configurations. We find $\langle S_n \rangle = 4.998$ MeV for the $n + {}^{235}\text{U}$ system, $\langle S_n \rangle = 4.915$ MeV for the $n + {}^{238}\text{U}$ system, and $\langle S_n \rangle = 5.375$ MeV for the $n + {}^{239}\text{Pu}$ system. For the range of incident neutron energies considered here, it is a reasonable approximation that the $\langle S_n \rangle$ values are constant, independent of the incident energy. Third, the average center-of-mass energies $\langle \varepsilon \rangle$ of the emitted prompt neutrons are calculated with the Los Alamos model [4]:

$$\langle \varepsilon \rangle = \frac{[P_{f_1}^A \bar{\nu}_{p_1} \langle \varepsilon_1 \rangle + P_{f_2}^A (\langle \xi_1 \rangle + \bar{\nu}_{p_2} \langle \varepsilon_2 \rangle) + P_{f_3}^A (\langle \xi_1 \rangle + \langle \xi_2 \rangle + \bar{\nu}_{p_3} \langle \varepsilon_3 \rangle)]}{[P_{f_1}^A \bar{\nu}_{p_1} + P_{f_2}^A (1 + \bar{\nu}_{p_2}) + P_{f_3}^A (2 + \bar{\nu}_{p_3})]}, \quad (24)$$

where, again, A is the mass number of the fissioning compound nucleus, the $P_{f_i}^A$ are the fission probabilities for i th-chance fission, the $\bar{\nu}_{p_i}$ are the average prompt neutron multiplicities for i th-chance fission, the ξ_i are the average kinetic energies of the evaporated neutrons prior to fission in 2nd-chance fission ($i = 1$) and 3rd-chance fission ($i = 2$), and the $\langle \varepsilon_i \rangle$ are the average center-of-mass neutron energies for i th-chance fission.

Eq. (24) has been evaluated as a function of incident neutron energy for the three systems under study and the results are shown in Fig. 9. One sees that the values of $\langle \varepsilon \rangle$ generally increase with increasing E_n , but decrease near 6 MeV and 13 MeV which are the approximate thresholds for 2nd- and 3rd-chance fission where the emission of 1 and 2 neutrons, respectively, prior to fission, reduce the fragment excitation energy available for neutron and gamma emission and, correspondingly, reduce $\langle \varepsilon \rangle$.

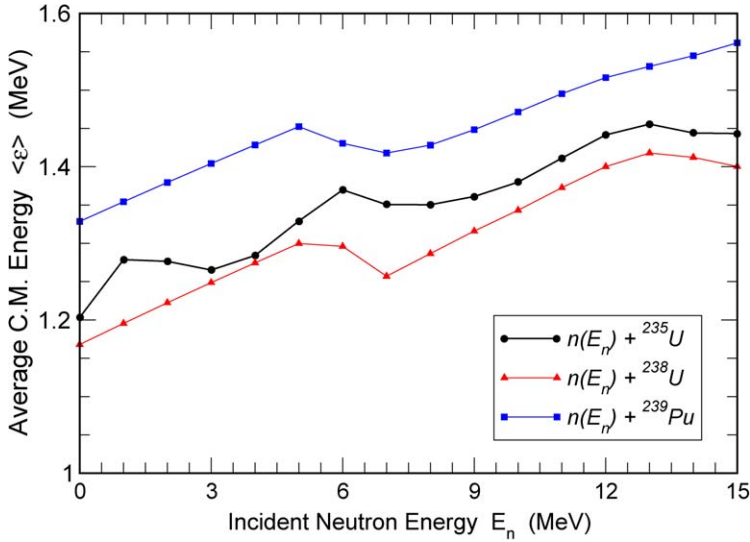


Fig. 9. Prompt fission neutron spectrum average center-of-mass energy (ε) for three systems calculated with the Los Alamos model (line segments are to guide the eye).

Note that the structure observed below ~ 3 MeV in the $n + {}^{235}\text{U}$ system is due to fits of the Los Alamos model to experimental spectra measured at these energies. It is clear from Figs. 8 and 9 that the $n + {}^{239}\text{Pu}$ system is the *hottest* of the three systems in terms of both the number of neutrons emitted and their energy, with the $n + {}^{235}\text{U}$ and $n + {}^{238}\text{U}$ systems very similar, but somewhat larger neutron emission energies for $n + {}^{235}\text{U}$.

Using the preceding information, Eq. (16) for the average fission-fragment excitation energy leading to prompt neutron emission (average total prompt neutron emission energy) can be evaluated for the three systems under study.

The results are shown in Fig. 10 which indicate an approximately linear dependence upon the incident neutron energy E_n and, again, more neutron emission for the Pu system and less, but comparable, emission for the two U systems.

Linear fits to the three calculations shown in Fig. 10 are illustrated in Figs. 11–13 together with the calculated points from Eq. (16) wherein the values of $\bar{\nu}_p(E_n)$ are taken from ENDF.

For the $n + {}^{235}\text{U}$ system:

$$\langle Ex_n^{\text{tot}} \rangle = 14.59 + 0.9772E_n \text{ (MeV)}. \quad (25)$$

For the $n + {}^{238}\text{U}$ system:

$$\langle Ex_n^{\text{tot}} \rangle = 14.11 + 0.9839E_n \text{ (MeV)}. \quad (26)$$

For the $n + {}^{239}\text{Pu}$ system:

$$\langle Ex_n^{\text{tot}} \rangle = 19.23 + 1.0707E_n \text{ (MeV)}. \quad (27)$$

3.3. Average total prompt gamma emission energy

The experimental data that we use for the $n + {}^{235}\text{U}$ system are those of Frehaut et al. (1982) [15] which are ratio measurements to the average total prompt gamma emission energy for

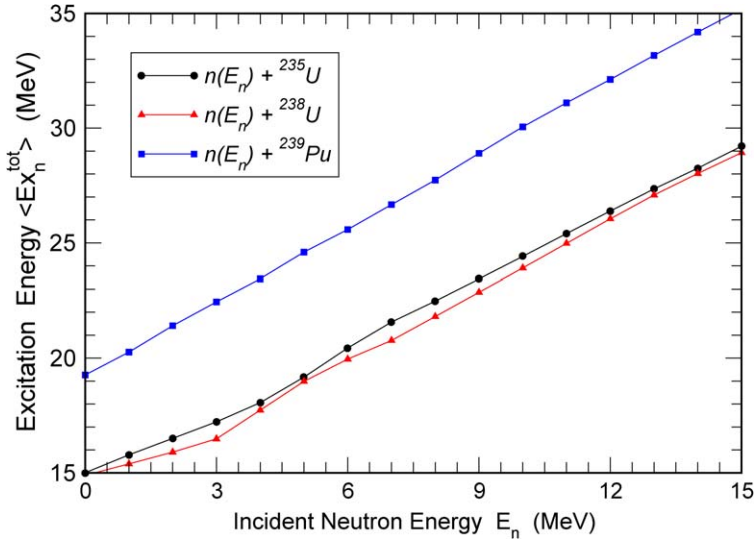


Fig. 10. Fission fragment excitation energy (Ex_n^{tot}) leading to prompt neutron emission for three systems from the Los Alamos model and ENDF (line segments are to guide the eye).

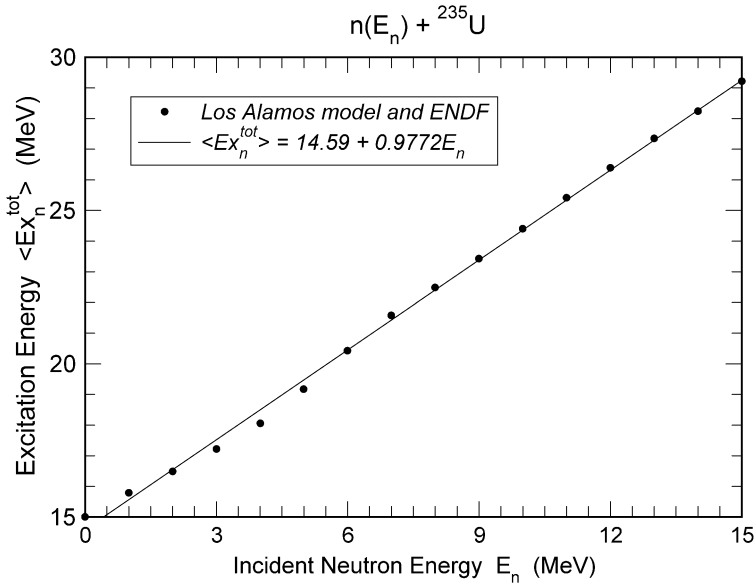


Fig. 11. Fission fragment excitation energy (Ex_n^{tot}) leading to prompt neutron emission in the $n(E_n) + {}^{235}\text{U}$ system.

${}^{252}\text{Cf(sf)}$. These ratio data have been converted back to absolute units by using the average of three measurements for ${}^{252}\text{Cf}$ reported in the Hoffman and Hoffman review [16]. The converted Frehaut et al. data are shown in Fig. 14 together with a linear fit to the data. There is nonlinear structure in these data, but for our present purposes we use the linear approximation.

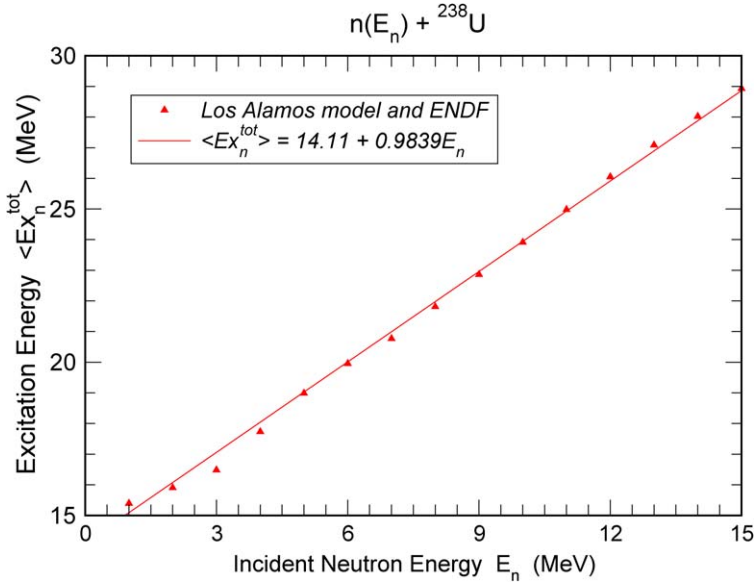


Fig. 12. Fission fragment excitation energy $\langle Ex_n^{\text{tot}} \rangle$ leading to prompt neutron emission in the $n(E_n) + {}^{238}\text{U}$ system.

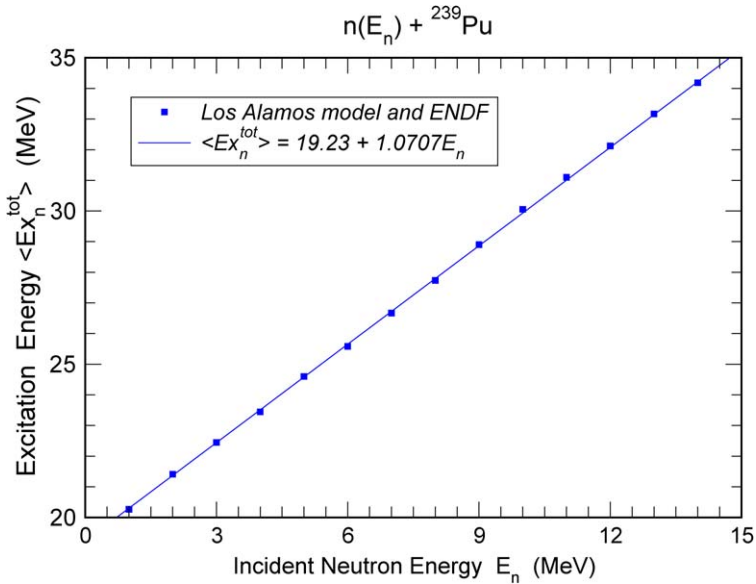


Fig. 13. Fission fragment excitation energy $\langle Ex_n^{\text{tot}} \rangle$ leading to prompt neutron emission in the $n(E_n) + {}^{239}\text{Pu}$ system.

For the $n + {}^{235}\text{U}$ system:

$$\langle E_\gamma^{\text{tot}} \rangle = (6.600 \pm 0.03) + (0.0777 \pm 0.004)E_n \text{ (MeV)}. \quad (28)$$

We have no experimental values for the average total prompt gamma emission energy in the $n + {}^{238}\text{U}$ system. Therefore, an empirical approach is used, namely, a linear assumption

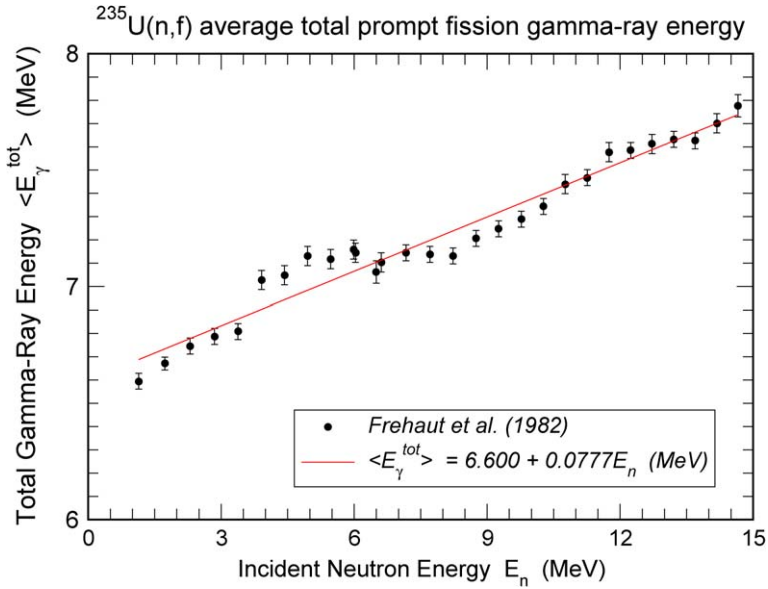


Fig. 14. Average total prompt fission gamma-ray energy (E_γ^{tot}) for the $n(E_n) + ^{235}\text{U}$ system.

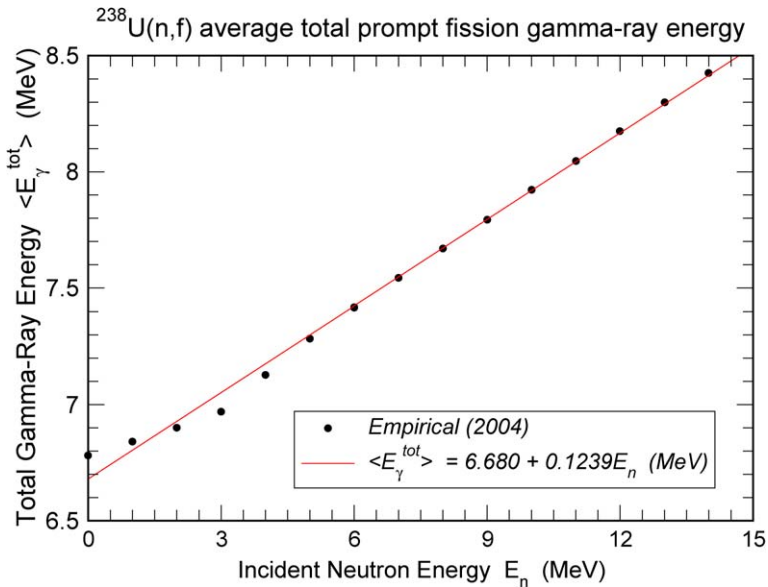


Fig. 15. Average total prompt fission gamma-ray energy (E_γ^{tot}) for the $n(E_n) + ^{238}\text{U}$ system.

with $\bar{\nu}_p(E_n)$ is made (based upon the Frehaut et al. [15] measurements) with the zero (thermal) energy value taken from the A -dependent fit by Hoffman and Hoffman [16], and the slope taken from that inferred by Frehaut et al. from the $n + ^{237}\text{Np}$ measurements that they performed. Note, however, that we use the lower experimental limit of their inferred slope because the $n + ^{237}\text{Np}$ system is *hotter* than that of $n + ^{238}\text{U}$. The resulting data points are labeled “Empirical (2004)” in Fig. 15 together with a linear fit in incident neutron energy.

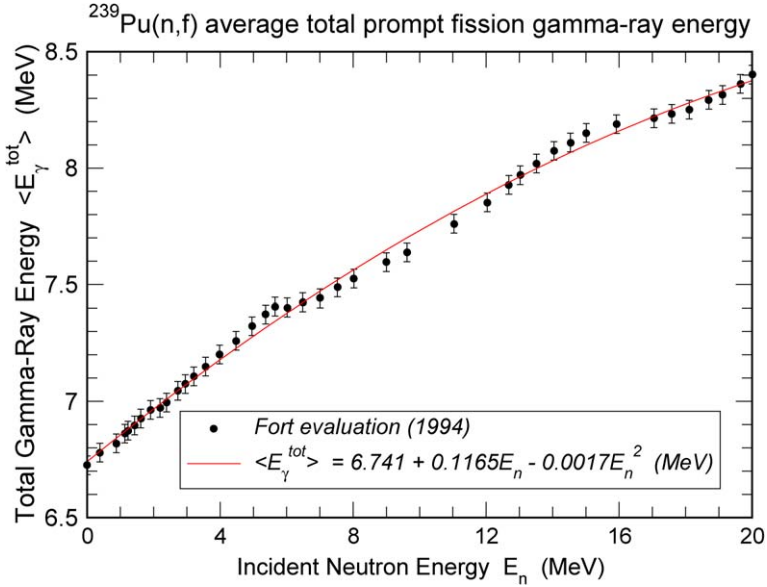


Fig. 16. Average total prompt fission gamma-ray energy $\langle E_\gamma^{\text{tot}} \rangle$ for the $n(E_n) + {}^{239}\text{Pu}$ system.

For the $n + {}^{238}\text{U}$ system:

$$\langle E_\gamma^{\text{tot}} \rangle = 6.6800 + 0.1239E_n \text{ (MeV)}. \quad (29)$$

Experimental values exist for the average total prompt gamma emission energy for the $n + {}^{239}\text{Pu}$ system, but only for thermal neutron energy: Pleasonton (1973) [17] measured a value of 6.73 ± 0.35 MeV for the thermal case. Direct measurements for greater neutron energy do not appear to exist.

Consequently, we employ an evaluation by Fort (1994) [18] which is based upon systematics with respect to the measurements by Frehaut et al. [15] on nearby actinides and upon multichance fission probabilities from the Japanese Nuclear Data Center. This evaluation is shown as the points appearing in Fig. 16 together with a quadratic fit in the incident neutron energy.

For the $n + {}^{239}\text{Pu}$ system:

$$\langle E_\gamma^{\text{tot}} \rangle = (6.741 \pm 0.02) + (0.1165 \pm 0.004)E_n - (0.0017 \pm 0.0002)E_n^2 \text{ (MeV)}. \quad (30)$$

4. Average total prompt fission energy release

Eq. (17) for the average total prompt energy release in fission can now be evaluated for the three systems under study:

For the $n + {}^{235}\text{U}$ system one substitutes Eqs. (18), (25), and (28) into Eq. (17), together with the value $B_n = 6.546$ MeV for this system, to obtain

$$\langle E_r \rangle = 185.6 - 0.0995E_n \text{ (MeV)}. \quad (31)$$

For the $n + {}^{238}\text{U}$ system one substitutes Eqs. (20), (26), and (29) into Eq. (17), together with the value $B_n = 4.806$ MeV for this system, to obtain

$$\langle E_r \rangle = 187.7 - 0.1318E_n + 0.0034E_n^2 \text{ (MeV)}. \quad (32)$$

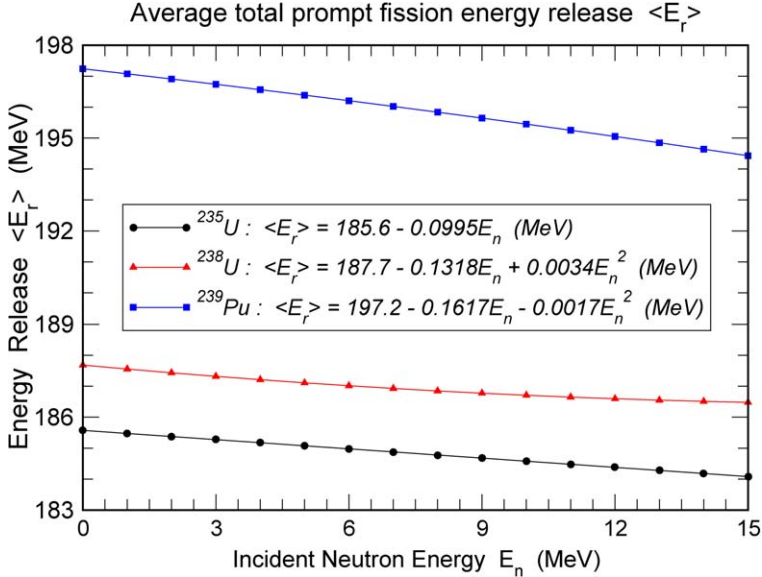


Fig. 17. Average total prompt fission energy release $\langle E_r \rangle$ for three systems.

For the $n + {}^{239}\text{Pu}$ system one substitutes Eqs. (22), (27), and (30) into Eq. (17), together with the value $B_n = 6.534$ MeV for this system, to obtain

$$\langle E_r \rangle = 197.2 - 0.1617E_n - 0.0017E_n^2 \text{ (MeV)}. \quad (33)$$

The calculated average total prompt fission energy release $\langle E_r \rangle$ for the three systems is shown in Fig. 17. There are two major features in this figure. First, the prompt energy release for the neutron-induced fission of ${}^{239}\text{Pu}$ is about 10 MeV greater than that of the two isotopes of U, over the entire energy range of 15 MeV, and the prompt energy release for the neutron-induced fission of ${}^{238}\text{U}$ is about 2 MeV greater than that of ${}^{235}\text{U}$, over the same energy range. Second, the prompt energy release decreases with increasing incident neutron energy for all three of the systems under study, which is contrary to intuition.

As already pointed out, this behavior is primarily due to the facts that symmetric fission increases with increasing neutron energy and that the total kinetic energy for symmetric fission is significantly less than the total kinetic energy for the more probable asymmetric fission. At the same time, however, the average prompt fission neutron multiplicities as a function of fission-fragment mass, $\bar{\nu}_p(A_f)$, are peaked for symmetric fission. Note that for far asymmetric fission (which is relatively infrequent) the total kinetic energy is also significantly reduced.

In the next section we examine the average total prompt energy deposition in the medium in which the fission event occurs, for the three systems under study.

5. Average total prompt fission energy deposition

The average total prompt fission energy deposition in the medium for binary fission $\langle E_d \rangle$ is defined as the average total prompt fission energy release in binary fission $\langle E_r \rangle$ plus the total energy brought to the fission event by the particle inducing the fission [the quantity $(E_n + B_n)$ for neutron-induced fission] minus the average total binding energy of the prompt neutrons emitted

by the fission fragments $\bar{v}_p \langle S_n \rangle$ [which is not deposited in the medium]. With this definition and Eq. (17) we obtain

$$\langle E_d \rangle = \langle E_r \rangle + (E_n + B_n) - \bar{v}_p \langle S_n \rangle \quad (34)$$

$$= \langle T_f^{\text{tot}} \rangle + \bar{v}_p \langle \varepsilon \rangle + \langle E_\gamma^{\text{tot}} \rangle. \quad (35)$$

We wish to express Eq. (35) in terms of laboratory observables in the medium. Therefore, note that Eq. (14) is of the form $\langle T_p^{\text{tot}} \rangle = \langle T_f^{\text{tot}} \rangle [1 - x]$ where x is a small quantity. Solving Eq. (14) for $\langle T_f^{\text{tot}} \rangle$ and performing an expansion of $1/[1 - x]$ yields

$$\langle T_f^{\text{tot}} \rangle = \langle T_p^{\text{tot}} \rangle \left[1 + \frac{\bar{v}_p}{2A} \left(\frac{\langle A_H \rangle}{\langle A_L \rangle} + \frac{\langle A_L \rangle}{\langle A_H \rangle} \right) \right]. \quad (36)$$

Inserting Eq. (36) into Eq. (35) and rearranging terms gives

$$\langle E_d \rangle = \langle T_p^{\text{tot}} \rangle + \langle E_{\text{neut}}^{\text{tot}} \rangle + \langle E_\gamma^{\text{tot}} \rangle \quad (37)$$

with $\langle E_{\text{neut}}^{\text{tot}} \rangle$ the average total prompt fission neutron kinetic energy in the laboratory system given by

$$\langle E_{\text{neut}}^{\text{tot}} \rangle = \bar{v}_p \left[\frac{1}{2} \left(\frac{\langle A_H \rangle}{\langle A_L \rangle} \frac{\langle T_f^{\text{tot}} \rangle}{A} + \frac{\langle A_L \rangle}{\langle A_H \rangle} \frac{\langle T_f^{\text{tot}} \rangle}{A} \right) + \langle \varepsilon \rangle \right] \quad (38)$$

$$= \bar{v}_p \left[\frac{1}{2} (\langle E_f^L \rangle + \langle E_f^H \rangle) + \langle \varepsilon \rangle \right] \quad (39)$$

$$= \bar{v}_p \langle E \rangle, \quad (40)$$

in which the prompt fission neutron spectrum average laboratory energy $\langle E \rangle$ is given by the Los Alamos model [4]

$$\langle E \rangle = \frac{1}{2} (\langle E_f^L \rangle + \langle E_f^H \rangle) + \langle \varepsilon \rangle, \quad (41)$$

and the approximation has been made in Eq. (38) that $\langle T_p^{\text{tot}} \rangle / A$ can be replaced by $\langle T_f^{\text{tot}} \rangle / A$ given that the $\langle A_{L,H} \rangle$ are not unique, but instead averages, and given that $\langle \varepsilon \rangle$ is the dominant term in the square brackets. In Eqs. (39) and (41) the quantities $\langle E_f^L \rangle$ and $\langle E_f^H \rangle$ are the average kinetic energies per nucleon of the moving light and heavy fission fragments, respectively, and are the quantities not included in $\langle E_{X_n}^{\text{tot}} \rangle$ as discussed in the beginning of Section 3.2.

Note that all averaged quantities appearing in Eqs. (37)–(41) depend upon the incident neutron energy E_n which has been suppressed for brevity. We use Eq. (37) for the average total prompt fission energy deposition for the remainder of this paper.

The evaluation of Eq. (40) for the three systems of interest is performed using the \bar{v}_p values from ENDF [5] shown in Fig. 8 and prompt fission neutron spectrum average laboratory energies $\langle E \rangle$ calculated for multi-chance fission with the Los Alamos model [4]:

$$\langle E \rangle = \frac{[P_{f_1}^A \bar{v}_{p_1} \langle E_1 \rangle + P_{f_2}^A (\langle \xi_1 \rangle + \bar{v}_{p_2} \langle E_2 \rangle) + P_{f_3}^A (\langle \xi_1 \rangle + \langle \xi_2 \rangle + \bar{v}_{p_3} \langle E_3 \rangle)]}{[P_{f_1}^A \bar{v}_{p_1} + P_{f_2}^A (1 + \bar{v}_{p_2}) + P_{f_3}^A (2 + \bar{v}_{p_3})]}, \quad (42)$$

where the $\langle E_i \rangle$ are the average laboratory neutron energies for i th-chance fission and all other quantities are defined as for Eq. (24).

The prompt fission neutron spectrum average laboratory energies $\langle E \rangle$ calculated with Eq. (42) for the three systems are shown in Fig. 18. Just as with the average center-of-mass energies $\langle \varepsilon \rangle$,

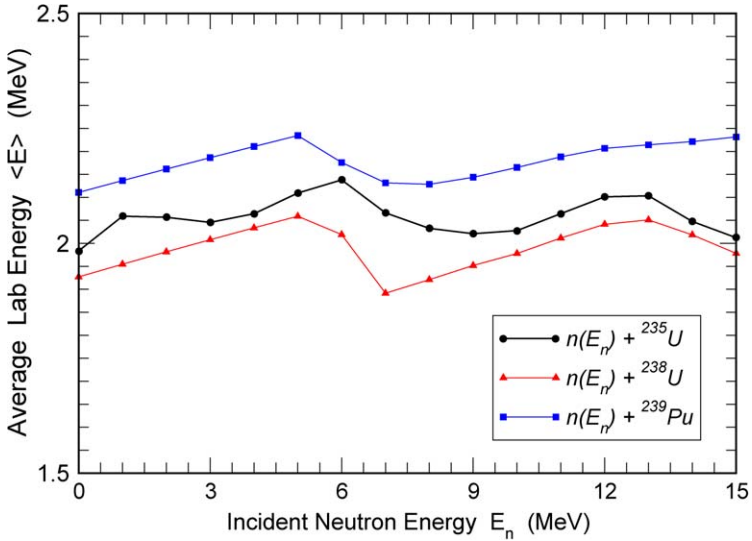


Fig. 18. Prompt fission neutron spectrum average laboratory energy $\langle E \rangle$ for three systems calculated with the Los Alamos model (line segments are to guide the eye).

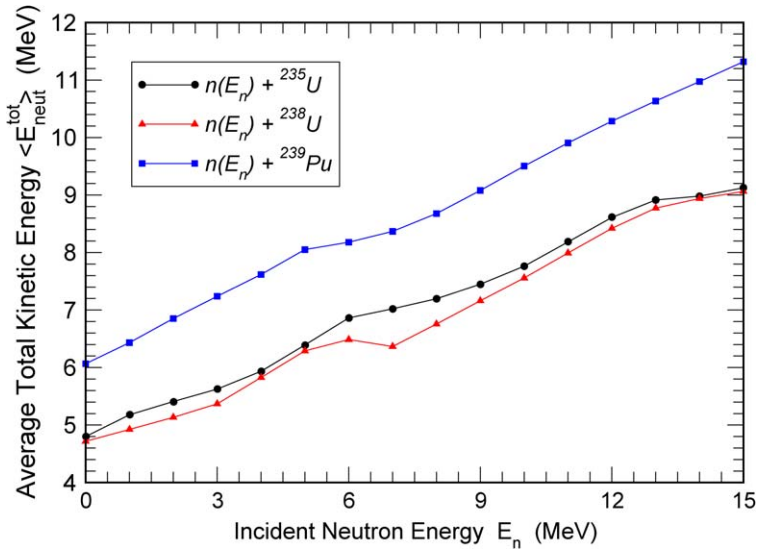


Fig. 19. Average total prompt fission neutron kinetic energy $\langle E_{\text{neut}}^{\text{tot}} \rangle$ for three systems from the Los Alamos model and ENDF (line segments are to guide the eye).

the values of $\langle E \rangle$ decrease near 6 MeV and 13 MeV, the approximate thresholds for 2nd- and 3rd-chance fission, and for the same reasons. The product of these two quantities $\langle E_{\text{neut}}^{\text{tot}} \rangle$ is shown as a function of incident neutron energy in Fig. 19 for the three systems of interest. Some evidence of multiple-chance fission threshold structure is still present.

Again, for our present purposes, we perform linear fits to the values of the average total prompt fission neutron kinetic energies $\langle E_{\text{neut}}^{\text{tot}} \rangle$ shown in Fig. 19 for the three systems. The results are

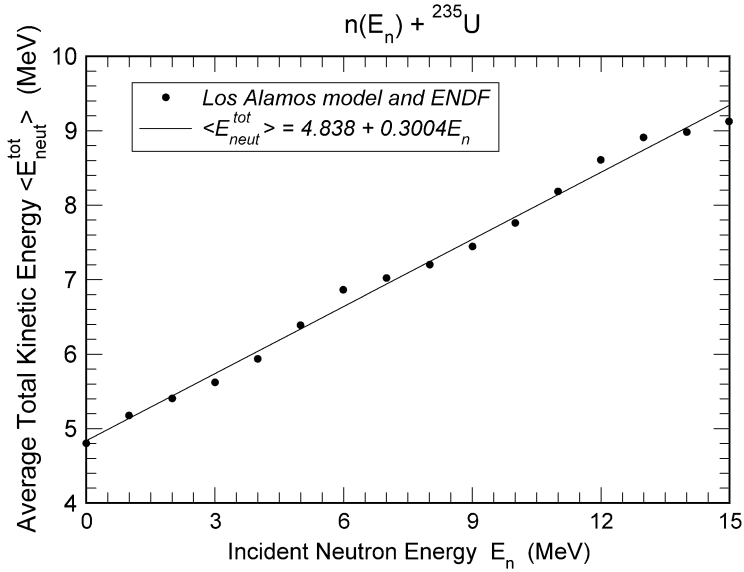


Fig. 20. Average total prompt fission neutron kinetic energy $\langle E_{neut}^{tot} \rangle$ for the $n(E_n) + {}^{235}\text{U}$ system.

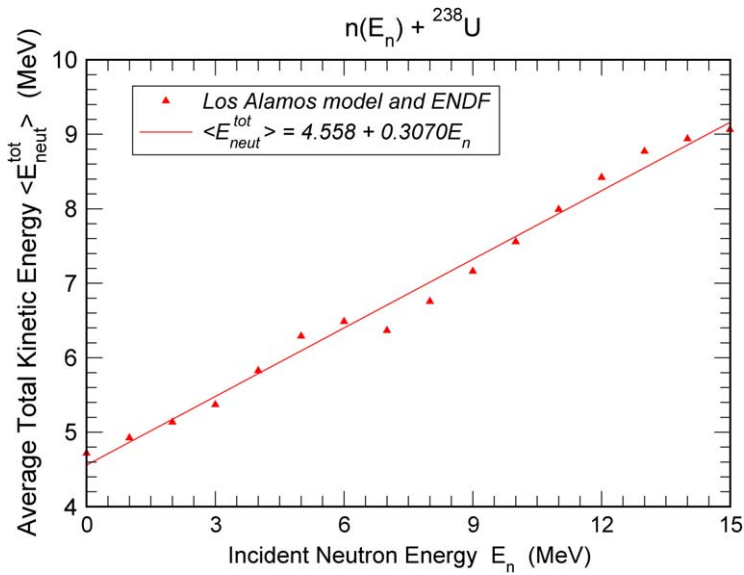


Fig. 21. Average total prompt fission neutron kinetic energy $\langle E_{neut}^{tot} \rangle$ for the $n(E_n) + {}^{238}\text{U}$ system.

shown together with the calculated values in Figs. 20–22.

For the $n + {}^{235}\text{U}$ system:

$$\langle E_{neut}^{tot} \rangle = 4.838 + 0.3004E_n \text{ (MeV)}. \tag{43}$$

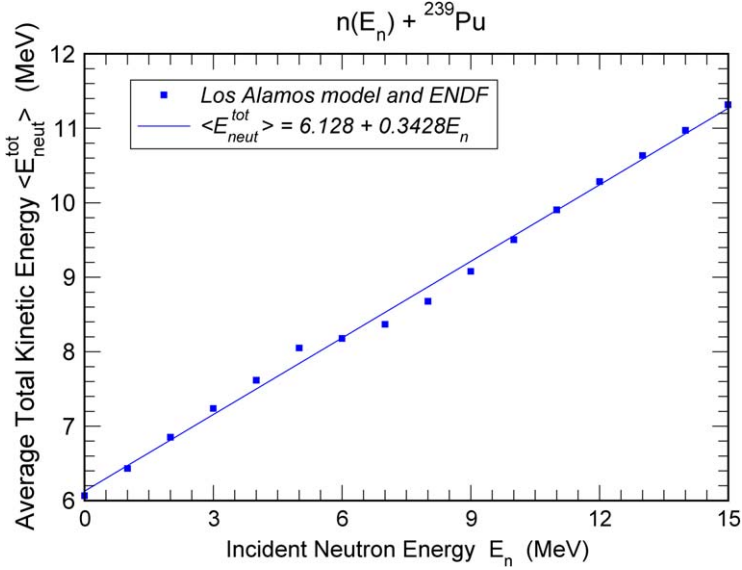


Fig. 22. Average total prompt fission neutron kinetic energy $\langle E_{\text{neut}}^{\text{tot}} \rangle$ for the $n(E_n) + {}^{239}\text{Pu}$ system.

For the $n + {}^{238}\text{U}$ system:

$$\langle E_{\text{neut}}^{\text{tot}} \rangle = 4.558 + 0.3070E_n \text{ (MeV)}. \quad (44)$$

For the $n + {}^{239}\text{Pu}$ system:

$$\langle E_{\text{neut}}^{\text{tot}} \rangle = 6.128 + 0.3428E_n \text{ (MeV)}. \quad (45)$$

Eq. (37) for the average total prompt fission energy deposition $\langle E_d \rangle$ can now be evaluated for the three systems under study:

For the $n + {}^{235}\text{U}$ system one substitutes Eqs. (19), (43), and (28) into Eq. (37) to obtain

$$\langle E_d \rangle = 180.57 + 0.1121E_n \text{ (MeV)}. \quad (46)$$

For the $n + {}^{238}\text{U}$ system one substitutes Eqs. (21), (44), and (29) into Eq. (37) to obtain

$$\langle E_d \rangle = 181.04 + 0.1079E_n + 0.0042E_n^2 \text{ (MeV)}. \quad (47)$$

For the $n + {}^{239}\text{Pu}$ system one substitutes Eqs. (23), (45), and (30) into Eq. (37) to obtain

$$\langle E_d \rangle = 188.42 + 0.0027E_n - 0.0017E_n^2 \text{ (MeV)}. \quad (48)$$

These three equations for the average total prompt fission energy deposition are shown as a function of incident neutron energy in Fig. 23. The energy dependence of $\langle E_d \rangle$ is weak, increasing slightly with incident neutron energy for the two U isotopes and decreasing very slightly for the Pu isotope. Again, the energy dependence is contrary to intuition and the explanation is the same as that for the energy release $\langle E_r \rangle$. However, the $\langle E_d \rangle$ energy dependence is stronger than that of $\langle E_r \rangle$ partly because the (positive) term $(E_n + B_n)$ wins over the (negative) term $\bar{\nu}_p \langle S_n \rangle$ in Eq. (34).

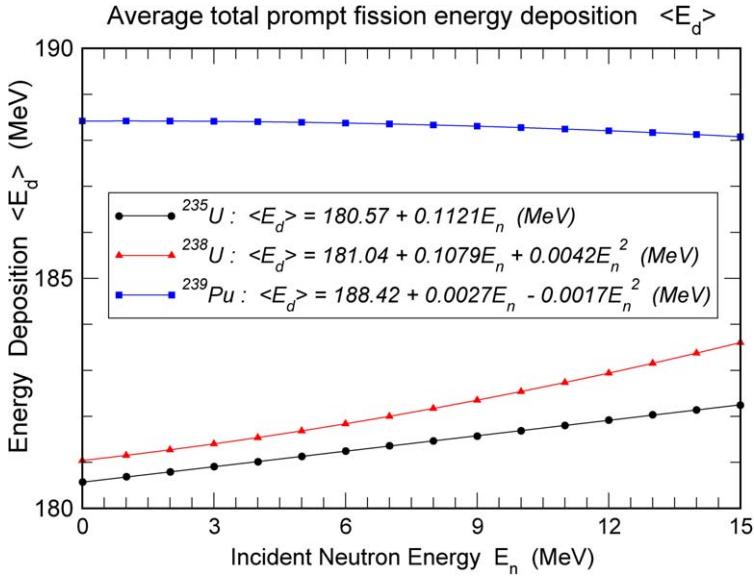


Fig. 23. Average total prompt fission energy deposition $\langle E_d \rangle$ for three systems.

6. Conclusions

The total prompt fission energy release and energy deposition, together with their components, have been determined as a function of the kinetic energy of the neutron inducing the fission, for ^{235}U , ^{238}U , and ^{239}Pu . This study has relied primarily upon existing (published) experimental measurements and secondarily upon nuclear theory and nuclear models.

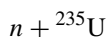
Contrary to basic physical intuition, it has been found that the energy release decreases somewhat with incident neutron energy and the energy deposition changes slightly with incident neutron energy. The main reason for this behavior is that symmetric fission increases with increasing incident neutron energy, but fission-fragment kinetic energies are at a minimum for symmetric fission. Even more striking is the fact that the Q values for fission are, on average, somewhat larger for symmetric fission than they are for asymmetric fission. The extra available fission-fragment excitation energy at symmetric fission, due to the smaller fragment kinetic energies and larger fission Q values, results in a peak in the $\bar{\nu}_p(A_f)$ vs. A_f curve, that is, the prompt neutron multiplicities are peaked at symmetric fission.

These results would become more physically correct with a number of more complete and more accurate measurements over the incident neutron energy range. Then, instead of the simple linear and quadratic energy dependencies used here, more realistic characterizations of the incident neutron energy dependencies could be performed, for example, near the thresholds for multi-chance fission. In the $n + ^{238}\text{U}$ system this could already be done for the average total fission product kinetic energy $\langle T_p^{\text{tot}} \rangle$, but is pointless to do so now because there are no measurements at all of the average total prompt fission gamma-ray energy $\langle E_\gamma^{\text{tot}} \rangle$ as a function of incident neutron energy for this same system. The current experimental data for fission product kinetic energies in the $n + ^{235}\text{U}$ and $n + ^{239}\text{Pu}$ systems allow, at best, linear energy dependencies.

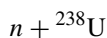
These results would also become more physically correct if the calculations performed using the Los Alamos model [4] were replaced by the identical calculations performed using a modern

Hauser–Feshbach approach. Here the competition between neutron and gamma emission from fission fragments would be treated exactly and the angular momentum dependencies would be treated for each particle type emission. However, such an approach does not yet exist because not enough is known to adequately specify the fission fragment initial conditions across the fragment mass and charge distributions. Namely, (a) the partition of fissioning compound nucleus excitation energy between the light and heavy fragments, (b) the fragment initial angular momenta, and (c) the fragment initial parities, must all be specified for approximately 400 fragments. In addition, the fragment mass and charge yield distributions must be known as a function of incident neutron energy in order to properly weight the approximately 400 Hauser–Feshbach results for each incident neutron energy. There does not yet exist a calculation of these yield distributions of sufficient accuracy to perform this task, and measured fission product mass and charge yield distributions allowing construction of the corresponding fragment distributions are sufficiently complete at only two incident neutron energies: thermal and 14 MeV.

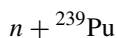
It is astonishing to find that after some 60 years of fission studies the post-scission fission observables for the three major actinides ^{235}U , ^{238}U , and ^{239}Pu have been so incompletely measured and understood. As a consequence of this work the following measurements are recommended for the three systems studied:



- (a) The average total fission-product kinetic energy should be measured from 10 keV to 30 MeV. The existing data stops at about 9 MeV and, furthermore, has uncertainties that need to be reduced.
- (b) The average total prompt fission gamma-ray energy should be measured from 15 MeV to 30 MeV and several (three) of Frehaut's data points between 1 and 15 MeV should be re-measured to verify the energy dependence.
- (c) The prompt fission neutron spectrum (out to 15 MeV emitted neutron energy) should be re-measured for incident neutron energies of 1, 2, 3, and 5 MeV, and measured for 4 MeV and the range 8 MeV to 30 MeV.



- (a) The average total prompt fission gamma-ray energy should be measured from 10 keV to 30 MeV. Apparently, no measurements exist.
- (b) The prompt fission neutron spectrum (out to 15 MeV emitted neutron energy) should be measured for incident neutron energies of 4, 10, and the range 12 to 30 MeV.



- (a) The average total fission-product kinetic energy should be measured from about 3 MeV to 30 MeV. The existing measurements become sparse at about 3.5 MeV and stop just beyond 5 MeV.
- (b) The average total prompt fission gamma-ray energy should be measured from 10 keV to 30 MeV. Only thermal measurements exist at the present time and the experimental content of Fort's evaluation [18] is unknown.
- (c) The prompt fission neutron spectrum (out to 15 MeV emitted neutron energy) should be measured for incident neutron energies ranging from 4 MeV to 30 MeV.

It is manifestly clear that measured components of the above quantities for the light and heavy mass peaks as well as for near symmetric and far asymmetric fission will be doubly useful in serving both fundamental and applied post-scission fission physics.

Appendix A. Multiple-chance fission equations

In the absence of the measured components of the average total prompt fission energy release $\langle E_r \rangle$ and average total prompt fission energy deposition $\langle E_d \rangle$ the following equations are used to calculate these quantities directly:

$$\langle E_r \rangle = \frac{[P_{f_1}^A \langle E_r(A) \rangle + P_{f_2}^A \langle E_r(A-1) \rangle + P_{f_3}^A \langle E_r(A-2) \rangle]}{[P_{f_1}^A + P_{f_2}^A + P_{f_3}^A]}, \quad (\text{A.1})$$

$$\langle E_d \rangle = \frac{[P_{f_1}^A \langle E_d(A) \rangle + P_{f_2}^A \langle E_d(A-1) \rangle + P_{f_3}^A \langle E_d(A-2) \rangle]}{[P_{f_1}^A + P_{f_2}^A + P_{f_3}^A]}, \quad (\text{A.2})$$

where the total fission probability P_f^A of the compound fissioning nucleus A at excitation energy $[E_n + B_n(A)]$ is given by

$$P_f^A [E_n + B_n(A)] = P_{f_1}^A [E_n + B_n(A)] + P_{f_2}^A [E_n + B_n(A)] + P_{f_3}^A [E_n + B_n(A)], \quad (\text{A.3})$$

in which $P_{f_1}^A$ is the probability for first-chance fission, the (n, f) reaction, $P_{f_2}^A$ is the probability for second-chance fission, the $(n, n' f)$ reaction, and $P_{f_3}^A$ is the probability for third-chance fission, the $(n, n' n'' f)$ reaction.

Correspondingly,

$$\langle E_r(A) \rangle = \langle T_f^{\text{tot}}(A) \rangle + \bar{\nu}_p(A) [\langle S_n(A) \rangle + \langle \epsilon_1(A) \rangle] + \langle E_\gamma^{\text{tot}}(A) \rangle - [E_n + B_n(A)], \quad (\text{A.4})$$

$$\langle E_d(A) \rangle = \langle T_p^{\text{tot}}(A) \rangle + \bar{\nu}_p(A) \langle E(A) \rangle + \langle E_\gamma^{\text{tot}}(A) \rangle, \quad (\text{A.5})$$

which are evaluated as a function of excitation energy $[E_n + B_n(A)]$ of the A system,

$$\langle E_r(A-1) \rangle = \langle T_f^{\text{tot}}(A-1) \rangle + \bar{\nu}_p(A-1) [\langle S_n(A-1) \rangle + \langle \epsilon_2(A-1) \rangle] + \langle E_\gamma^{\text{tot}}(A-1) \rangle - [E_n - \langle \xi_1(A) \rangle], \quad (\text{A.6})$$

$$\langle E_d(A-1) \rangle = \langle T_p^{\text{tot}}(A-1) \rangle + \bar{\nu}_p(A-1) \langle E(A-1) \rangle + \langle E_\gamma^{\text{tot}}(A-1) \rangle, \quad (\text{A.7})$$

which are evaluated as a function of excitation energy $[E_n - \langle \xi_1(A) \rangle]$ of the $A-1$ system, and

$$\langle E_r(A-2) \rangle = \langle T_f^{\text{tot}}(A-2) \rangle + \bar{\nu}_p(A-2) [\langle S_n(A-2) \rangle + \langle \epsilon_3(A-2) \rangle] + \langle E_\gamma^{\text{tot}}(A-2) \rangle - [E_n - \langle \xi_1(A) \rangle - \langle \xi_2(A-1) \rangle - B_n(A-1)], \quad (\text{A.8})$$

$$\langle E_d(A-2) \rangle = \langle T_p^{\text{tot}}(A-2) \rangle + \bar{\nu}_p(A-2) \langle E(A-2) \rangle + \langle E_\gamma^{\text{tot}}(A-2) \rangle, \quad (\text{A.9})$$

which are evaluated as a function of excitation energy $[E_n - \langle \xi_1(A) \rangle - \langle \xi_2(A-1) \rangle - B_n(A-1)]$ of the $A-2$ system.

All quantities appearing in the equations of this appendix are defined elsewhere in the text, mostly near Eq. (24) and Eqs. (41), (42).

References

- [1] I. Halpern, *Annu. Rev. Nucl. Sci.* 9 (1959) 245.
- [2] F. Gönnenwein, in: C. Wagemans (Ed.), *The Nuclear Fission Process*, CRC Press, Boca Raton, FL, 1991, p. 287.
- [3] L. Wilets, *Theories of Nuclear Fission*, Clarendon, Oxford, 1964, pp. 21–22.
- [4] D.G. Madland, J.R. Nix, *Nucl. Sci. Eng.* 81 (1982) 213.
- [5] *Evaluated Nuclear Data File (ENDF)*, National Nuclear Data Center, Brookhaven National Laboratory, Upton, NY.
- [6] C. Wagemans, in: C. Wagemans (Ed.), *The Nuclear Fission Process*, CRC Press, Boca Raton, FL, 1991, p. 545.
- [7] J.W. Meadows, C. Budtz-Jorgensen, Argonne National Laboratory report ANL/NDM-64, 1982.
- [8] Ch. Straede, C. Budtz-Jorgensen, H.-H. Knitter, *Nucl. Phys. A* 462 (1987) 85.
- [9] R. Müller, et al., *Phys. Rev. C* 29 (1984) 885.
- [10] C.M. Zöller, Investigation of the neutron-induced fission of ^{238}U in the energy range 1 MeV to 500 MeV, Ph.D. thesis, Technische Hochschule Darmstadt, Darmstadt, Germany, 1995 (unpublished). Note that these experimental data are available from the Nuclear Data Section of the IAEA, Vienna.
- [11] F. Vivès, F.-J. Hamsch, H. Bax, S. Oberstedt, *Nucl. Phys. A* 662 (2000) 63.
- [12] N.I. Akimov, et al., *Sov. J. Nucl. Phys.* 13 (1971) 272.
- [13] H.W. Schmitt, J.H. Neiler, F.J. Walter, *Phys. Rev.* 141 (1966) 1146.
- [14] J.H. Neiler, F.J. Walter, H.W. Schmitt, *Phys. Rev.* 149 (1966) 894.
- [15] J. Frehaut, A. Bertin, R. Bois, in: *Proceedings of International Conference on Nuclear Data for Science and Technology*, Antwerp, Belgium, 6–10 September 1982, Reidel, Dordrecht, Holland, 1983, p. 78.
- [16] D.C. Hoffman, M.M. Hoffman, *Annu. Rev. Nucl. Sci.* 24 (1974) 151.
- [17] F. Pleasonton, *Nucl. Phys. A* 213 (1973) 413.
- [18] E. Fort, private communications, 1994, 2004.